JOINT 2-D DOA TRACKING FOR MULTIPLE MOVING TARGETS USING ADAPTIVE FREQUENCY ESTIMATION

Jun Liu and Xiangqian Liu

Department of Electrical and Computer Engineering
University of Louisville, Louisville, KY 40292

ABSTRACT

In this paper, we propose a low-complexity adaptive two-dimensional (2-D) frequency estimation algorithm to jointly track 2-D direction-of-arrivals (DOAs) of multiple moving targets with a uniform rectangular array (URA). The LOAFR1 subspace tracking algorithm is applied to estimate the signal subspace recursively, then an adaptive eigenvector-based frequency estimation approach is used to resolve the 2-D DOAs from the estimated signal subspace. The eigenvectors are obtained from the eigen-decomposition of an adaptively weighted matrix, whose weighting factors are updated according to the current DOA estimates and the optimization criterion derived from the perturbation analysis to minimize estimation error variance. The complexity order of the proposed algorithm is analyzed in detail to demonstrate its low computation cost, and the tracking performance is validated by simulation results.

Index Terms— Frequency estimation, adaptive signal processing, multidimensional signal processing, localization, tracking

1. INTRODUCTION

The problem of tracking the direction-of-arrivals (DOAs) of multiple moving targets in radar signal processing has attracted much interests in recent years. Various methods based on adaptive filter and Bayesian statistics were proposed [8]. However, most previous work assumed that the DOAs were one dimension vectors. A uniform rectangular array (URA) can be applied to track the DOAs in two dimensions: elevation and azimuth. The problem to jointly estimate the two dimensional (2-D) angles is actually a 2-D frequency estimation problem. How to effectively associate the 2-D angles of the same target is critical. The Unitary ESPRIT algorithm was applied to jointly estimate 2-D DOAs in [9]. Based on simultaneous Schur decomposition, the Unitary ESPRIT algorithm was generalized to multidimensional case in [2]. The problem to jointly track 2-D DOA was considered in [7], where a subspace tracking algorithm (i.e., Bi-SVD) was applied to track the subspaces of the structural matrices in an adaptive MI-ESPRIT algorithm. The MI-ESPRIT algorithm employed adaptive simultaneous Schur decomposition to estimate the 2-D DOAs.

Recently multidimensional frequency estimation based on eigenvectors was proposed in [5]. This approach avoids the expensive computational cost of simultaneous Schur decomposition and demonstrates superior performance in simulation experiments. We analyzed the performance of eigenvector-based frequency estimation algorithms and proposed an optimization strategy for such algorithms in [4] using adjustable weighting factors.

This material is based on work supported by the U.S. Army Research Laboratory and the U.S. Army Research Office under grant number W911NF-05-1-0485.

In this paper, we propose a new 2-D DOA tracking algorithm based on our previous work in frequency estimation. Similar to [7], we use subspace tracking to estimate the instantaneous signal subspace, but we adopt another subspace tracking algorithm – LOAFR1 [6], since the LOAFR1 algorithm demonstrates better performance over other subspace tracking algorithms and has the same complexity order as the remaining steps of our algorithm. The signal subspace shares the same column space as that of a structural matrix, which is the Khatri-Rao product of several Vandermonde matrices. The transformation matrix connecting the structural matrix and the signal subspace is estimated through a so-called "weighted diagonalization" method, which performs eigenvalue decomposition (EVD) of an adaptively weighted matrix. The weighting factors are updated adaptively according to current angle estimates and an optimization criterion similar to that of [4]. The sequential quadratic programming (SQP) process in [4] is avoided here, thus computational complexity is reduced. The computational order of the proposed tracking algorithm is as low as $\mathcal{O}(MNF^2)$, where M and N are the dimension sizes of the URA array in elevation and azimuth directions, F is the number of targets. It can be used to estimate the 2-D DOA of multiple moving targets at every snapshot and track the DOA trajectories in real time. The performance of the proposed algorithm is evaluated by numerical simulations.

In the following, upper (lower) bold face letters are used for matrices (column vectors). $\boldsymbol{A}^T$, $\boldsymbol{A}^H$, and $\boldsymbol{A}^\dagger$ denote the transpose, Hermitian transpose, and pseudo-inverse of $\boldsymbol{A}$, respectively. We will use $\otimes$ for the Kronecker product, $\odot$ for the Khatri-Rao product, $\boldsymbol{I}_p$ for a $p \times p$ identity matrix, $\mathbf{0}_{M\times N}$ for an $M \times N$ zero matrix, $\boldsymbol{D}(\boldsymbol{a})$ for a diagonal matrix with $\boldsymbol{a}$ as its diagonal, and $a_{f,n}$ or $[\boldsymbol{A}]_{f,n}$ for the (f, n)-th element of $\boldsymbol{A}$.

2. THE PROPOSED 2-D DOA TRACKING ALGORITHM

In this paper, we assume that the number of targets does not change in the tracking process. Suppose there are F moving targets that are to be tracked by a URA of size $M \times N$. Suppose the elevation and azimuth angles of the f-th target at tth snapshot are $\theta_f(t)$ and $\phi_f(t)$, which are the angles with respect with x-axis and y-axis; the inter-sensor spacings in x-axis and y-axis are Δ_x and Δ_y, respectively. Define

$$\omega_f(t) = \frac{2\pi}{\lambda}\Delta_x \cos\theta_f(t), \quad \nu_f(t) = \frac{2\pi}{\lambda}\Delta_y \cos\phi_f(t), \quad (1)$$

where λ is the wavelength. The output signal of the URA at the (m, n)-th sensor is modeled as [9]

$$x_{m,n}(t) = \sum_{f=1}^{F} c_f(t) e^{j(m-1)\omega_f(t)} e^{j(n-1)\nu_f(t)}, \; t = 1, \ldots, T,$$

where $m = 1, \ldots, M$ and $n = 1, \ldots, N$. If we choose $\Delta_x = \Delta_y = \frac{\lambda}{2}$, and assume $0 < \theta_f(t), \phi_f(t) \leq \pi$, there is one-to-one mapping between $\omega_f(t)$ and $\theta_f(t)$, and between $\nu_f(t)$ and $\phi_f(t)$, where $-\pi \leq \omega_f(t) < \pi$ and $-\pi \leq \nu_f(t) < \pi$. For this reason, in the following we also refer $\omega_f(t)$ and $\phi_f(t)$ as the 2-D DOA of the f-th target.

If the f-th target moves, $(\omega_f(t), \nu_f(t))$ travels a trajectory in the $\Pi \times \Pi$ plane, where $\Pi = [-\pi, \pi)$. The problem of 2-D DOA tracking is to estimate F trajectories $\{(\omega_f(t), \nu_f(t))\}_{f=1}^F$ from the observations $\{x_{m,n}(t)\}$ for $t = 1, \ldots, T$. Define the snapshot vector as

$$\boldsymbol{x}(t) = [x_{1,1}(t)\ x_{1,2}(t)\ \cdots\ x_{1,N}(t)\ x_{2,1}(t)\ \cdots\ x_{M,N}(t)]^T,$$

and the amplitude vector $\boldsymbol{c}(t) := [c_1(t)\ c_2(t)\ \cdots\ c_F(t)]^T$, then it can be verified that

$$\boldsymbol{x}(t) = \big(\boldsymbol{A}(t) \odot \boldsymbol{B}(t)\big)\boldsymbol{c}(t) = \boldsymbol{G}(t)\boldsymbol{c}(t), \quad t = 1, \ldots, T, \tag{2}$$

where $\boldsymbol{A}(t)$ and $\boldsymbol{B}(t)$ are Vandermonde matrices with generators $\{e^{j\omega_f(t)}\}_{f=1}^F$ and $\{e^{j\nu_f(t)}\}_{f=1}^F$ respectively, and the structural matrix $\boldsymbol{G}(t) := \boldsymbol{A}(t) \odot \boldsymbol{B}(t)$. Suppose that the signal subspace of the time-varying correlation matrix of $\boldsymbol{x}(t)$ is $\boldsymbol{Q}(t)$, then $\boldsymbol{Q}(t)$ and $\boldsymbol{G}(t)$ share the same column space, therefore there exists a nonsingular transformation matrix $\boldsymbol{T}(t)$ of size $F \times F$ such that

$$\boldsymbol{G}(t) = \boldsymbol{Q}(t)\boldsymbol{T}(t). \tag{3}$$

The proposed fast recursive 2-D frequency tracking has four steps: firstly, apply the LOAFR1 algorithm to estimate the signal subspace $\boldsymbol{Q}(t)$; secondly, estimate the transformation matrix $\boldsymbol{T}(t)$ by performing EVD to an adaptive weighted matrix; then, obtain the estimates of $\boldsymbol{G}(t)$ through (3) and estimate the 2-D DOAs by dividing the elements in $\boldsymbol{G}(t)$; finally, update the weighting factors according to the current estimates of DOA. The updated weighting factors are applied to estimate $\boldsymbol{T}(t+1)$ in the next snapshot. We describe the proposed algorithm in detail in the following.

2.1. Subspace Tracking Based on the LOAFR1 Algorithm

We adopt the LOAFR1 subspace tracking algorithm [6] to estimate the signal subspace $\boldsymbol{Q}(t)$ from $\boldsymbol{x}(t)$ adaptively. The initialization process of the LOAFR1 algorithm is

$$\boldsymbol{Q}(0) = \begin{bmatrix} \boldsymbol{I}_F \\ \boldsymbol{0}_{(MN-F)\times F} \end{bmatrix}, \quad \boldsymbol{P}(0) = \begin{bmatrix} \boldsymbol{I}_F \\ \boldsymbol{0}_{(MN-F)\times F} \end{bmatrix},$$
$$\boldsymbol{\Theta}(0) = \boldsymbol{I}_F, \quad \rho = 0.85.$$

At time t, the updating process of the LOAFR1 algorithm is

$$\boldsymbol{h}(t) = \boldsymbol{Q}^H(t-1)\boldsymbol{x}(t), \tag{4}$$
$$\boldsymbol{P}(t) = \rho\boldsymbol{P}(t-1)\boldsymbol{\Theta}(t-1) + (1-\rho)\boldsymbol{x}(t)\boldsymbol{h}^H(t), \tag{5}$$
$$\boldsymbol{Q}(t)\boldsymbol{L}(t) = \boldsymbol{P}(t), \quad \text{by truncated QR factorization}, \tag{6}$$
$$\boldsymbol{\Theta}(t) = \boldsymbol{Q}^H(t-1)\boldsymbol{Q}(t). \tag{7}$$

2.2. Estimation of the Transformation Matrix $\boldsymbol{T}(t)$

In the following, we use a recently developed method [4], which is called "weighted diagonalization", to solve for $\boldsymbol{T}(t)$. We construct a matrix pencil along the elevation dimension of $\boldsymbol{Q}(t)$ such that

$$\boldsymbol{U}_{1,1}(t) := \left(\left[\boldsymbol{I}_{M-1}\ \boldsymbol{0}_{(M-1)\times 1}\right] \otimes \boldsymbol{I}_N\right)\boldsymbol{Q}(t), \tag{8}$$
$$\boldsymbol{U}_{1,2}(t) := \left(\left[\boldsymbol{0}_{(M-1)\times 1}\ \boldsymbol{I}_{M-1}\right] \otimes \boldsymbol{I}_N\right)\boldsymbol{Q}(t). \tag{9}$$

Then, it can be verified that

$$\boldsymbol{M}_1(t) := \boldsymbol{U}_{1,1}^{\dagger}(t)\boldsymbol{U}_{1,2}(t) = \boldsymbol{T}^{-1}(t)\boldsymbol{D}\big(\boldsymbol{\omega}(t)\big)\boldsymbol{T}(t),$$

where $\boldsymbol{\omega}(t) := \left[e^{j\omega_1(t)}\ e^{j\omega_2(t)}\ \cdots\ e^{j\omega_F(t)}\right]^T$. Similarly we construct a matrix pencil along the azimuth dimension of $\boldsymbol{Q}(t)$ such that

$$\boldsymbol{U}_{2,1}(t) := \left(\boldsymbol{I}_M \otimes \left[\boldsymbol{I}_{N-1}\ \boldsymbol{0}_{(N-1)\times 1}\right]\right)\boldsymbol{Q}(t), \tag{10}$$
$$\boldsymbol{U}_{2,2}(t) := \left(\boldsymbol{I}_M \otimes \left[\boldsymbol{0}_{(N-1)\times 1}\ \boldsymbol{I}_{N-1}\right]\right)\boldsymbol{Q}(t), \tag{11}$$

and it can be verified that

$$\boldsymbol{M}_2(t) := \boldsymbol{U}_{2,1}^{\dagger}(t)\boldsymbol{U}_{2,2}(t) = \boldsymbol{T}^{-1}(t)\boldsymbol{D}(\boldsymbol{\nu}(t))\boldsymbol{T}(t),$$

where $\boldsymbol{\nu}(t) := \left[e^{j\nu_1(t)}\ e^{j\nu_2(t)}\ \cdots\ e^{j\nu_F(t)}\right]^T$. We introduce two variable complex weighting factors $\alpha_1(t-1)$ and $\alpha_2(t-1)$, which are initialized randomly and updated adaptively according to Section 2.4. Consider the EVD of the following weighted matrix

$$\boldsymbol{M}(t) := \alpha_1(t-1)\boldsymbol{M}_1(t) + \alpha_2(t-1)\boldsymbol{M}_2(t) \tag{12}$$
$$= \boldsymbol{T}^{-1}(t)\boldsymbol{D}(\boldsymbol{\zeta}(t))\boldsymbol{T}(t), \tag{13}$$

where $\boldsymbol{\zeta}(t) := [\zeta_1(t)\ \zeta_2(t)\ \cdots\ \zeta_F(t)]^T$, and

$$\zeta_f(t) := \alpha_1(t-1)e^{j\omega_f(t)} + \alpha_2(t-1)e^{j\nu_f(t)}, \tag{14}$$

for $f = 1, \ldots, F$. Consider the column scaling and permutation ambiguity, the eigen-decomposition of $\boldsymbol{M}(t)$ of (13) gives

$$\boldsymbol{T}_{\rm sp}(t) := \boldsymbol{T}\boldsymbol{\Lambda}(t)\boldsymbol{\Delta}(t), \tag{15}$$

where $\boldsymbol{\Lambda}(t)$ is a nonsingular diagonal column scaling matrix and $\boldsymbol{\Delta}(t)$ is a permutation matrix.

2.3. Estimation of DOAs

Once the transformation matrix $\boldsymbol{T}_{\rm sp}(t)$ is obtained, we estimate $\boldsymbol{G}(t)$ according to (c.f. (3)) $\boldsymbol{G}_{\rm sp}(t) = \boldsymbol{Q}(t)\boldsymbol{T}_{\rm sp}(t)$. Since $\boldsymbol{G}(t) = \boldsymbol{A}(t) \odot \boldsymbol{B}(t)$, the elevation and azimuth angles of the same target appear in the same column of $\boldsymbol{G}(t)$. Thanks to this structure, we can obtain the exponentials containing $\{\omega_f(t)\}$ and $\{\nu_f(t)\}$ by dividing suitably chosen elements of the columns of $\boldsymbol{G}_{\rm sp}(t)$. Therefore the column scaling will not have material effect on the algorithm. Since there are many quotients that can be regarded as the estimate of the exponentials, we take average over them to reduce estimation error variance in the case when the observation is noisy. This method is the so called "circular mean" in direction statistics. However, because of the existence of the permutation ambiguity $\boldsymbol{\Delta}(t)$, the order of estimated angles is different from the true order in (2). Suppose the elevation and azimuth angles of the g-th target appear in the f-th column of $\boldsymbol{G}_{\rm sp}(t)$, then $e^{j\omega_g(t)}$ can be estimated by

$$e^{j\omega_g(t)} = \frac{1}{(M-1)N}\sum_{n=N+1}^{MN}\frac{g_{n,f}(t)}{g_{n-N,f}(t)}, \quad f, g \in \{1, \ldots, F\}. \tag{16}$$

where $g_{n,f}(t)$ is the (n, f)-th element of $\boldsymbol{G}_{\rm sp}(t)$. Similarly, $e^{j\nu_g(t)}$ can be estimated by

$$e^{j\nu_g(t)} = \frac{1}{M(N-1)}\sum_{\substack{n=2 \\ \mathrm{mod}\ (n,N)\neq 1}}^{MN}\frac{g_{n,f}(t)}{g_{n-1,f}(t)}, \quad f, g \in \{1, \ldots, F\}. \tag{17}$$

Finally $\omega_g(t)$ and $\nu_g(t)$ of the g-th target can be obtained by

$$\omega_g(t) = \mathcal{I}\left(\log e^{j\omega_g(t)}\right), \quad \nu_g(t) = \mathcal{I}\left(\log e^{j\nu_g(t)}\right), \tag{18}$$

where $\mathcal{I}(\cdot)$ stands for the imaginary part.

2.4. Update of the Weighting Factors

Similar to [4], the weighting factors $\alpha_1(t-1)$ and $\alpha_2(t-1)$ in (12) can be optimized so that the performance of eigenvector-based estimation can be improved. However the optimization algorithm (i.e., SQP) used in [4] is computational demanding and not suitable for a tracking algorithm. Here we propose a low-complexity method to dynamically adjust the weighting factors. If we assume $|\alpha_i(t)| \leq 0.5$, for $i = 1, 2$, then it is obvious that $|\zeta_f(t)| \leq 1$, for $f = 1, \ldots, F$. For the EVD in (13), it is shown in [5] that the perturbation of the f-th eigenvector $\boldsymbol{t}_f(t)$ is

$$\Delta \boldsymbol{t}_f(t) = \boldsymbol{T}(t)\boldsymbol{D}_f(t)\boldsymbol{T}^{-1}(t)\Delta\boldsymbol{M}(t)\boldsymbol{t}_f(t), \qquad (19)$$

where $\boldsymbol{D}_f(t)$ is diagonal matrix with $[\boldsymbol{D}_f(t)]_{f,f} = 0$ and $[\boldsymbol{D}_f(t)]_{g,g} = \frac{1}{\zeta_f(t)-\zeta_g(t)}$ for $g \neq f$. In order to minimize the estimation errors, we should minimize the perturbation $\Delta\boldsymbol{T}(t)$ and thus the norm of all $\boldsymbol{D}_f(t)$, $f = 1, \ldots, F$. Therefore we propose to solve the following optimization problem

$$\boldsymbol{\zeta}_{\text{opt}}(t) = \arg\min_{\boldsymbol{\zeta}(t)} \Gamma(\boldsymbol{\zeta}(t)), \quad |\zeta_f(t)| \leq 1, f = 1, \ldots, F. \quad (20)$$

$$\Gamma(\boldsymbol{\zeta}(t)) := \sum_{f=1}^{F} \sum_{\substack{g=1 \\ g\neq f}}^{F} \frac{1}{|\zeta_f(t) - \zeta_g(t)|}. \qquad (21)$$

It can be verified that $\Gamma(\boldsymbol{\zeta}(t)) \leq F(F-1)\frac{1}{\beta(\boldsymbol{\zeta}(t))}$, where

$$\beta(\boldsymbol{\zeta}(t)) = \min_{\substack{g=1 \\ g\neq f}} |\zeta_f(t) - \zeta_g(t)|. \qquad (22)$$

In order to solve (20), we can maximize $\beta(\boldsymbol{\zeta}(t))$. If $F \leq 6$, it is easy to prove that the optimal $\{\zeta_f(t)\}_{f=1}^{F}$ should distribute regularly in the unit circle such that

$$\boldsymbol{\zeta}_{\text{opt}} = \left[1\ e^{j2\pi/F}\ \cdots\ e^{j2\pi(F-1)/F}\right]^T. \qquad (23)$$

For $F > 6$, the problem is related to the circle packing problem and solved in [3]. If we define $\boldsymbol{\alpha}(t) := [\alpha_1(t)\ \alpha_2(t)]^T$, since $\boldsymbol{\omega}(t)$ and $\boldsymbol{\nu}(t)$ change continuously, at time $t+1$, Eqn. (14) become

$$\boldsymbol{\zeta}(t+1) = \left[\ \boldsymbol{\omega}(t+1)\ \ \boldsymbol{\nu}(t+1)\ \right]\boldsymbol{\alpha}(t) \approx \left[\ \boldsymbol{\omega}(t)\ \ \boldsymbol{\nu}(t)\ \right]\boldsymbol{\alpha}(t) \quad (24)$$

In order to make $\boldsymbol{\zeta}(t+1)$ close to the optimal distribution as in (23), we update $\boldsymbol{\alpha}(t)$ by solving following least-squares (LS) problem

$$\boldsymbol{\alpha}(t) = \arg\min_{\boldsymbol{\alpha}} \left\| \left[\ \boldsymbol{\omega}(t)\ \ \boldsymbol{\nu}(t)\ \right]\boldsymbol{\alpha} - \boldsymbol{\zeta}_{\text{opt}} \right\|. \qquad (25)$$

The updated $\boldsymbol{\alpha}(t)$ is employed in (12) at time $t+1$.

Since the DOA of one target vary continuous, we can eliminate the permutation ambiguity $\boldsymbol{\Delta}(t)$ and associate the DOA estimate at time t with those at time $t-1$ by minimizing the difference of the exponentials at time t and those at time $t-1$

$$\boldsymbol{p}_o = \arg\min_{\boldsymbol{p}} \Big\{ \sum_{f=1}^{F} \Big[\left| e^{j\omega_{p(f)}(t)} - e^{j\omega_f(t-1)} \right|^2 + \left| e^{j\nu_{p(f)}(t)} - e^{j\nu_f(t-1)} \right|^2 \Big] \Big\},$$

Here $\boldsymbol{p} = \{p(1)\ p(2)\ \cdots\ p(F)\}$ is a permutation of $\{1\ 2\ \cdots\ F\}$. $e^{j\omega_{p(f)}(t)}$ and $e^{j\nu_{p(f)}(t)}$ are the estimates at time t obtained in (16) and (17) respectively. We append the current DOA estimate to the DOA trajectory as $\omega_f(t) = \omega_{p_o(f)}(t)$ and $\nu_f(t) = \nu_{p_o(f)}(t)$.

We count the consumed flops of the proposed algorithm in Table 1. In practise, we use Gauss elimination to solve the equation $\boldsymbol{U}_{1,1}^H(t)\boldsymbol{U}_{1,1}(t)\boldsymbol{X} = \boldsymbol{U}_{1,1}^H(t)\boldsymbol{U}_{2,1}(t)$ to obtain $\boldsymbol{M}_1(t)$. The method of normal equations [1] is employed to solve the LS problem (25).

Table 1. The complexity order of the proposed algorithm

Algorithm Operations	Complexity Order
$\boldsymbol{h}(t) = \boldsymbol{Q}^H(t-1)\boldsymbol{x}(t)$ in (4)	MNF
Updating $\boldsymbol{P}(t)$ as (5)	$MNF^2 + MNF + F^2$
QR factorization to $\boldsymbol{P}(t)$	$2MNF^2$
$\boldsymbol{\Theta}(t) = \boldsymbol{Q}^H(t-1)\boldsymbol{Q}(t)$ in (7)	MNF^2
$\boldsymbol{M}_1(t) = \boldsymbol{U}_{1,1}^{\dagger}(t)\boldsymbol{U}_{1,2}(t)$	$2MNF^2 + 8F^3/3$
$\boldsymbol{M}_2(t) = \boldsymbol{U}_{2,1}^{\dagger}(t)\boldsymbol{U}_{2,2}(t)$	$2MNF^2 + 8F^3/3$
EVD of $\boldsymbol{M}(t)$	$25F^3$
$\boldsymbol{G}(t) = \boldsymbol{Q}(t)\boldsymbol{T}(t)$	MNF^2
Estimation of $e^{\omega_g(t)}$ by (16)	$(M-1)NF$
Estimation of $e^{\nu_g(t)}$ by (17)	$M(N-1)F$
$\min \left\| [\boldsymbol{\omega}(t)\ \ \boldsymbol{\nu}(t)]\,\boldsymbol{\alpha}(t) - \boldsymbol{\zeta}_{\text{opt}} \right\|$	$4F$
Total	$9MNF^2 + 30F^3$

3. SIMULATION RESULTS

In this section, we present the simulation results. We consider three moving targets, whose DOAs vary as linear functions of time. Therefore $\omega_f(t)$ and $\nu_f(t)$ are sinusoidal functions of time. The size of the URA is 10×10. The observation signal from the array is polluted by complex additive white Gaussian noise (AWGN), i.e., Eqn. (2) becomes

$$\boldsymbol{x}(t) = \boldsymbol{G}(t)\boldsymbol{c}(t) + \boldsymbol{n}(t),$$

where $\boldsymbol{n}(t)$ is noise with variance σ^2. The signal-to-noise ratio (SNR) is defined as $\text{SNR} = -10\log_{10}\sigma^2$. The sampling period is $T_s = 0.1$ ms and the tracking duration is from 0 s to 0.1 s, therefore there are $T = 1000$ snapshots. The amplitudes $\{c_f(t)\}_{t=1}^{T}$ are drawn from independent normal distributions.

Fig. 1 illustrates the true and estimated DOA trajectories of the moving targets in the $\Pi \times \Pi$ plane at $\text{SNR} = 2$dB for 5 noise realizations. The point in the plane with coordinates $(\omega_f(t), \nu_f(t))$ represents the 2-D DOA of the f-th target at time t. As time elapses, these points form three trajectory curves that describe the variation of the 2-D DOAs of the three moving targets. As we can see from Fig. 1, the estimated trajectories match well to the true trajectories. In Fig. 2 and Fig. 3, we plot the variation of the elevation and azimuth angles, respectively, as functions of time in the unit of T_s at $\text{SNR} = 2$dB for 5 noise realizations. These results demonstrate that the proposed algorithm can track the 2-D DOA variations closely.

We also evaluate the performance of the proposed algorithm in various SNRs through Monte Carlo simulation. The scenario is the same as the previous experiment except that the number of snapshot is $T = 200$. For comparison, we also simulate another 2-D frequency tracking algorithm by combining the LOAFR1 subspace tracking [6] and the 2-D Unitary ESPRIT algorithm [9], which we call "LOAFR1 + 2D Unitary ESPRIT". Different from our proposed algorithm, this algorithm uses the 2-D Unitary ESPRIT algorithm to estimate $(\omega_f(t), \nu_f(t))$ from $\boldsymbol{Q}(t)$. The normalized mean square error (NMSE) is defined as

$$\text{NMSE} = \frac{1}{2FT}\sum_{t=1}^{T}\sum_{f=1}^{F}\left[\left|\frac{\widehat{\omega}_f(t) - \omega_f(t)}{\omega_f(t)}\right|^2 + \left|\frac{\widehat{\nu}_f(t) - \nu_f(t)}{\nu_f(t)}\right|^2\right],$$

where $\widehat{\omega}_f(t)$ and $\widehat{\nu}_f(t)$ are estimated DOAs. We average the NMSE over 1000 realizations and plot the NMSE of the two algorithms in Fig. 4. It is evident that our proposed algorithm outperforms the

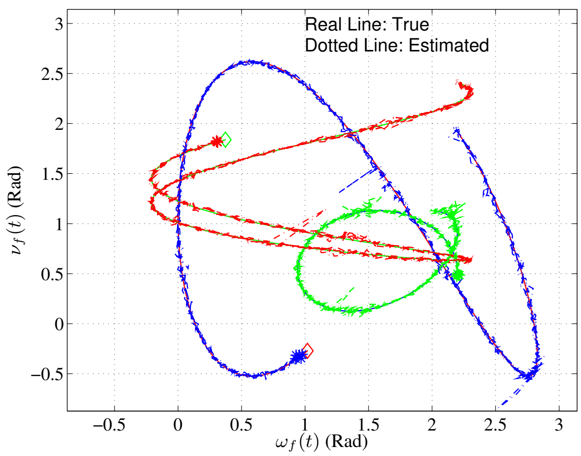

Fig. 1. The trajectory of the true and estimated 2-D DOAs for three moving targets (SNR = 2dB)

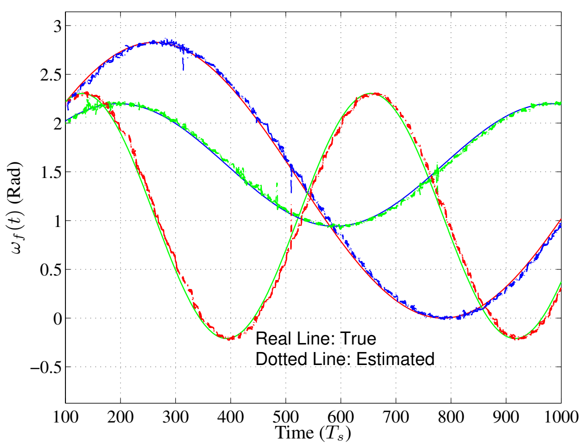

Fig. 2. The true and estimated elevation angles for three moving targets (SNR = 2dB)

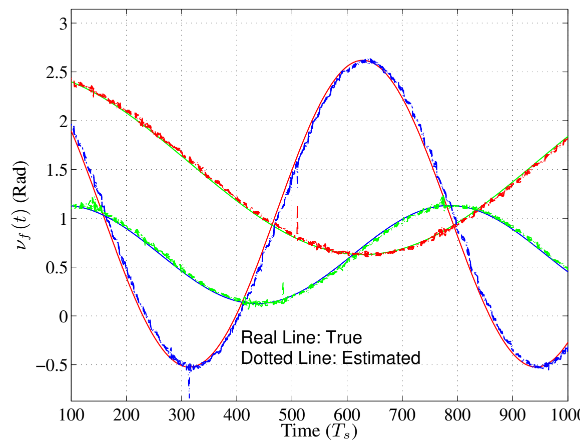

Fig. 3. The true and estimated azimuth angles for three moving targets (SNR = 2dB)

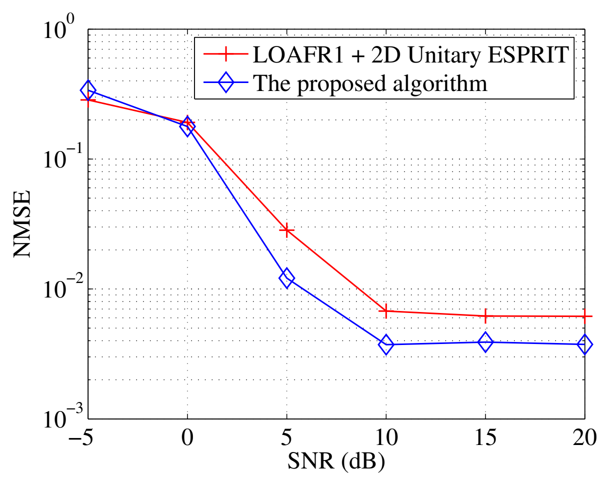

Fig. 4. The NMSE versus SNR

"LOAFR1 + 2D Unitary ESPRIT" algorithm in moderate and high SNR range in Fig. 4. This demonstrates the advantage of the proposed adaptive weighted diagonalization scheme since the subspace tracking steps of the two algorithms are identical. Notice that in the high SNR range the floor of NMSE implies these two trackers are both biased estimators due to the estimation delay.

An interesting problem under investigation is the tracking of multiple moving targets when the signal powers fluctuate as the targets move, and the number of signals may also vary. For example, if the number of targets varies, an adaptive order selection approach similar to that of [6] may be considered, and the least squares problem (25) also changes.

4. REFERENCES

[1] G. H. Golub and C. F. Van Loan, *Matrix Computation*, 3rd Ed., John Hopkins University Press, 1996.

[2] M. Haardt and J. A. Nossek, "Simultaneous Schur decomposition of several nonsymmetric matrices to achieve automatic pairing in multidimensional harmonic retrieval problems," *IEEE Trans. Signal Processing*, vol. 46, no. 1, pp. 161–169, Jan. 1998.

[3] S. Kravitz, "Packing cylinders into cylindrical containers," *Mathematics Magazine,* vol. 40, no.2, pp. 65–71, Mar. 1967.

[4] J. Liu and X. Liu, "Optimizing eigenvector based frequency estimation in the presence of identical frequencies in multiple dimensions," *Proc. SPAWC,* Cannes, France, Jul. 2–5, 2006.

[5] J. Liu and X. Liu, "An eigenvector based algebraic approach for multidimensional frequency estimation with improved identifiability," *IEEE Trans. Signal Processing*, vol. 54, no. 12, pp. 4543–4556, Dec. 2006.

[6] P. Strobach, "Low-rank adaptive filter," *IEEE Trans. Signal Processing,* vol. 44, no. 12, pp. 2932–2947, Dec. 1996.

[7] P. Strobach, "Bi-iteration multiple invariance subspace tracking and adaptive ESPRIT," *IEEE Trans. Signal Processing,* vol. 48, no. 2, pp. 442–456, Feb. 2000.

[8] J. Xin and A. Sano, "Efficient subspace-based algorithm for adaptive bearing estimation and tracking," *IEEE Trans. Signal Processing,* vol 53, no. 12, pp 4485–4505, Dec. 2005.

[9] M. D. Zoltowski, M. Haardt and C. P. Mathews, "Close-form 2-D angle estimation with rectangular arrays in element space or Beamspace via Unitary ESPRIT," *IEEE Trans. Signal Processing,* vol. 44, no. 2, pp. 316–328, Feb. 1996.